



University Transportation Research Center - Region 2

# Final Report



## Accelerated Aging of Asphalt by UV-Oxidation

Performing Organization: Manhattan College



June 2018



Sponsor:  
University Transportation Research Center - Region 2

## University Transportation Research Center - Region 2

The Region 2 University Transportation Research Center (UTRC) is one of ten original University Transportation Centers established in 1987 by the U.S. Congress. These Centers were established with the recognition that transportation plays a key role in the nation's economy and the quality of life of its citizens. University faculty members provide a critical link in resolving our national and regional transportation problems while training the professionals who address our transportation systems and their customers on a daily basis.

The UTRC was established in order to support research, education and the transfer of technology in the field of transportation. The theme of the Center is "Planning and Managing Regional Transportation Systems in a Changing World." Presently, under the direction of Dr. Camille Kamga, the UTRC represents USDOT Region II, including New York, New Jersey, Puerto Rico and the U.S. Virgin Islands. Functioning as a consortium of twelve major Universities throughout the region, UTRC is located at the CUNY Institute for Transportation Systems at The City College of New York, the lead institution of the consortium. The Center, through its consortium, an Agency-Industry Council and its Director and Staff, supports research, education, and technology transfer under its theme. UTRC's three main goals are:

### Research

The research program objectives are (1) to develop a theme based transportation research program that is responsive to the needs of regional transportation organizations and stakeholders, and (2) to conduct that program in cooperation with the partners. The program includes both studies that are identified with research partners of projects targeted to the theme, and targeted, short-term projects. The program develops competitive proposals, which are evaluated to insure the most responsive UTRC team conducts the work. The research program is responsive to the UTRC theme: "Planning and Managing Regional Transportation Systems in a Changing World." The complex transportation system of transit and infrastructure, and the rapidly changing environment impacts the nation's largest city and metropolitan area. The New York/New Jersey Metropolitan has over 19 million people, 600,000 businesses and 9 million workers. The Region's intermodal and multimodal systems must serve all customers and stakeholders within the region and globally. Under the current grant, the new research projects and the ongoing research projects concentrate the program efforts on the categories of Transportation Systems Performance and Information Infrastructure to provide needed services to the New Jersey Department of Transportation, New York City Department of Transportation, New York Metropolitan Transportation Council, New York State Department of Transportation, and the New York State Energy and Research Development Authority and others, all while enhancing the center's theme.

### Education and Workforce Development

The modern professional must combine the technical skills of engineering and planning with knowledge of economics, environmental science, management, finance, and law as well as negotiation skills, psychology and sociology. And, she/he must be computer literate, wired to the web, and knowledgeable about advances in information technology. UTRC's education and training efforts provide a multidisciplinary program of course work and experiential learning to train students and provide advanced training or retraining of practitioners to plan and manage regional transportation systems. UTRC must meet the need to educate the undergraduate and graduate student with a foundation of transportation fundamentals that allows for solving complex problems in a world much more dynamic than even a decade ago. Simultaneously, the demand for continuing education is growing – either because of professional license requirements or because the workplace demands it – and provides the opportunity to combine State of Practice education with tailored ways of delivering content.

### Technology Transfer

UTRC's Technology Transfer Program goes beyond what might be considered "traditional" technology transfer activities. Its main objectives are (1) to increase the awareness and level of information concerning transportation issues facing Region 2; (2) to improve the knowledge base and approach to problem solving of the region's transportation workforce, from those operating the systems to those at the most senior level of managing the system; and by doing so, to improve the overall professional capability of the transportation workforce; (3) to stimulate discussion and debate concerning the integration of new technologies into our culture, our work and our transportation systems; (4) to provide the more traditional but extremely important job of disseminating research and project reports, studies, analysis and use of tools to the education, research and practicing community both nationally and internationally; and (5) to provide unbiased information and testimony to decision-makers concerning regional transportation issues consistent with the UTRC theme.

### Project No(s):

UTRC/RF Grant No: 49198-18-28

### Project Date:

June 2018

### Project Title:

Accelerated Aging of Asphalt by UV-Oxidation

### Project's Website:

<http://www.utrc2.org/research/projects/accelerated-aging-asphalt-uv-oxidation>

### Principal Investigator(s):

**Daniel Hochstein, Ph.D.**

Assistant Professor

Civil & Environmental Engineering

Manhattan College

4513 Manhattan College Parkway

Riverdale, NY 10471

Tel: (212) 862-7177

Email: [daniel.hochstein@manhattan.edu](mailto:daniel.hochstein@manhattan.edu)

### Performing Organization(s):

Manhattan College

### Sponsor(s):

University Transportation Research Center (UTRC)

To request a hard copy of our final reports, please send us an email at [utrc@utrc2.org](mailto:utrc@utrc2.org)

### Mailing Address:

University Transportation Research Center

The City College of New York

Marshak Hall, Suite 910

160 Convent Avenue

New York, NY 10031

Tel: 212-650-8051

Fax: 212-650-8374

Web: [www.utrc2.org](http://www.utrc2.org)

## Board of Directors

The UTRC Board of Directors consists of one or two members from each Consortium school (each school receives two votes regardless of the number of representatives on the board). The Center Director is an ex-officio member of the Board and The Center management team serves as staff to the Board.

### City University of New York

*Dr. Robert E. Paaswell - Director Emeritus of NY*  
*Dr. Hongmian Gong - Geography/Hunter College*

### Clarkson University

*Dr. Kerop D. Janoyan - Civil Engineering*

### Columbia University

*Dr. Raimondo Betti - Civil Engineering*  
*Dr. Elliott Sclar - Urban and Regional Planning*

### Cornell University

*Dr. Huaizhu (Oliver) Gao - Civil Engineering*  
*Dr. Richard Geddes - Cornell Program in Infrastructure Policy*

### Hofstra University

*Dr. Jean-Paul Rodrigue - Global Studies and Geography*

### Manhattan College

*Dr. Anirban De - Civil & Environmental Engineering*  
*Dr. Matthew Volovski - Civil & Environmental Engineering*

### New Jersey Institute of Technology

*Dr. Steven I-Jy Chien - Civil Engineering*  
*Dr. Jyoung Lee - Civil & Environmental Engineering*

### New York Institute of Technology

*Dr. Nada Marie Anid - Engineering & Computing Sciences*  
*Dr. Marta Panero - Engineering & Computing Sciences*

### New York University

*Dr. Mitchell L. Moss - Urban Policy and Planning*  
*Dr. Rae Zimmerman - Planning and Public Administration*

### (NYU Tandon School of Engineering)

*Dr. John C. Falcocchio - Civil Engineering*  
*Dr. Kaan Ozbay - Civil Engineering*  
*Dr. Elena Prassas - Civil Engineering*

### Rensselaer Polytechnic Institute

*Dr. José Holguín-Veras - Civil Engineering*  
*Dr. William "Al" Wallace - Systems Engineering*

### Rochester Institute of Technology

*Dr. James Winebrake - Science, Technology and Society/Public Policy*  
*Dr. J. Scott Hawker - Software Engineering*

### Rowan University

*Dr. Yusuf Mehta - Civil Engineering*  
*Dr. Beena Sukumaran - Civil Engineering*

### State University of New York

*Michael M. Fancher - Nanoscience*  
*Dr. Catherine T. Lawson - City & Regional Planning*  
*Dr. Adel W. Sadek - Transportation Systems Engineering*  
*Dr. Shmuel Yahalom - Economics*

### Stevens Institute of Technology

*Dr. Sophia Hassiotis - Civil Engineering*  
*Dr. Thomas H. Wakeman III - Civil Engineering*

### Syracuse University

*Dr. Baris Salman - Civil Engineering*  
*Dr. O. Sam Salem - Construction Engineering and Management*

### The College of New Jersey

*Dr. Thomas M. Brennan Jr - Civil Engineering*

### University of Puerto Rico - Mayagüez

*Dr. Ismael Pagán-Trinidad - Civil Engineering*  
*Dr. Didier M. Valdés-Díaz - Civil Engineering*

## UTRC Consortium Universities

The following universities/colleges are members of the UTRC consortium under MAP-21 ACT.

City University of New York (CUNY)  
Clarkson University (Clarkson)  
Columbia University (Columbia)  
Cornell University (Cornell)  
Hofstra University (Hofstra)  
Manhattan College (MC)  
New Jersey Institute of Technology (NJIT)  
New York Institute of Technology (NYIT)  
New York University (NYU)  
Rensselaer Polytechnic Institute (RPI)  
Rochester Institute of Technology (RIT)  
Rowan University (Rowan)  
State University of New York (SUNY)  
Stevens Institute of Technology (Stevens)  
Syracuse University (SU)  
The College of New Jersey (TCNJ)  
University of Puerto Rico - Mayagüez (UPRM)

## UTRC Key Staff

**Dr. Camille Kamga:** *Director, Associate Professor of Civil Engineering*

**Dr. Robert E. Paaswell:** *Director Emeritus of UTRC and Distinguished Professor of Civil Engineering, The City College of New York*

**Dr. Ellen Thorson:** *Senior Research Fellow*

**Penny Eickemeyer:** *Associate Director for Research, UTRC*

**Dr. Alison Conway:** *Associate Director for Education/Associate Professor of Civil Engineering*

**Nadia Aslam:** *Assistant Director for Technology Transfer*

**Nathalie Martinez:** *Research Associate/Budget Analyst*

**Andriy Blagay:** *Graphic Intern*

**Tierra Fisher:** *Office Manager*

**Dr. Sandeep Mudigonda,** *Research Associate*

**Dr. Rodrigue Tchamna,** *Research Associate*

**Dr. Dan Wan,** *Research Assistant*

**Bahman Moghimi:** *Research Assistant;  
Ph.D. Student, Transportation Program*

**Sabiheh Fagigh:** *Research Assistant;  
Ph.D. Student, Transportation Program*

**Patricio Vicuna:** *Research Assistant  
Ph.D. Candidate, Transportation Program*

TECHNICAL REPORT STANDARD TITLE PAGE

1. Report No.	2. Government Accession No.	3. Recipient's Catalog No.	
4. Title and Subtitle  <b>Accelerated Aging of Asphalt by UV-Oxidation</b>		5. Report Date  <b>June, 2018</b>	
		6. Performing Organization Code	
7. Author(s) <b>Daniel Hochstein, PhD</b>		8. Performing Organization Report No.	
9. Performing Organization Name and Address <b>Manhattan College 4513 Manhattan College Parkway Riverdale, NY 10471</b>		10. Work Unit No.	
		11. Contract or Grant No. <b>49198-18-28</b>	
12. Sponsoring Agency Name and Address <b>University Transportation Research Center Marshak Hall - Science Building, Suite 910 The City College of New York 138th Street &amp; Convent Avenue, New York, NY 10031</b>		13. Type of Report and Period Covered <b>Final, Sept. 1, 2016 - Sept 6, 2018</b>	
		14. Sponsoring Agency Code	
15. Supplementary Notes			
16. Abstract  <p>The aging of asphalt binder due to UV-oxidation is a phenomenon that affects the durability and performance of asphalt pavements. This report documents results of accelerated laboratory UV-oxidation tests that have been conducted. Thin-film asphalt binder samples have been oxidized using fluorescent UVA and UVB lamps, and the degree of oxidation was determined by measuring the rotational viscosity of the aged binder. The results show that the viscosity increases with the UV-exposure time. This indicates that rotational viscosity is a suitable method to track the UV-oxidative aging of asphalt and validates its use in further studies of this phenomenon. Additionally two UV-aging models were fitted to the experimental results.</p>			
17. Key Words <b>Asphalt, Oxidation, Accelerated Aging, UV</b>		18. Distribution Statement	
19. Security Classif (of this report)  <b>Unclassified</b>	20. Security Classif. (of this page)  <b>Unclassified</b>	21. No of Pages  <b>34</b>	22. Price

**Disclaimer**

The contents of this report reflect the views of the authors, who are responsible for the facts and the accuracy of the information presented herein. The contents do not necessarily reflect the official views or policies of the UTRC. This report does not constitute a standard, specification or regulation. This document is disseminated under the sponsorship of the US Department of Transportation, University Transportation Centers Program, in the interest of information exchange. The U.S. Government assumes no liability for the contents or use thereof.

## Table of Contents

List of Figures.....	2
List of Tables .....	2
Executive Summary .....	3
1. Background and Literature Review .....	4
1.1. Solar Radiation .....	5
1.2. Asphalt Oxidation .....	7
1.3. Accelerated Photooxidation of Asphalt Binder .....	10
1.4. Modeling UV-Oxidation of Asphalt Binder .....	11
1.5. Asphalt Aging Models.....	13
2. Materials and Methods .....	16
2.1. Preparation of Asphalt Binder Specimens .....	16
2.2. UV Exposure .....	17
2.3. Rotational Viscosity of Aged/Unaged Asphalt Binder .....	18
3. Laboratory Aging Tests .....	19
3.1. Aging Index vs. Time .....	19
3.2. UVA vs. UVB .....	20
3.3. Effect of Sample Thickness .....	21
3.4. Reciprocity of Time/Intensity.....	23
4. Estimation of the In-Service UV Radiation Dose .....	24
4.1. UV Irradiance for Selected US Cities .....	25
4.2. Correlation between Laboratory and In-Service UV Aging .....	28
5. Conclusions.....	29
References .....	32

## List of Figures

Figure 1: Reference Solar Spectral Irradiance .....	6
Figure 2: NDD Model .....	15
Figure 3: FRCR Model (Y-Axis is $\Delta \log \eta$ ).....	16
Figure 4: FRCR Model (Y-Axis is AI) .....	16
Figure 5: Asphalt Specimen after Masking Tape is Removed.....	17
Figure 6: UV Lamp Spectral Distribution.....	18
Figure 7: Experimental Results .....	21
Figure 8: NDD and FRCR Models Fitted to Experimental Results .....	21
Figure 9: Aging Index for UVA and UVB .....	22
Figure 10: Aging Index for Different Sample Thicknesses .....	23
Figure 11: Noon Spectral GHI for LGA .....	25
Figure 12: Spectral UV GHI from a TMY in NYC - 6/21 .....	27
Figure 13: Spectral UV GHI from a TMY in NYC - 12/21 .....	27
Figure 14: Total UV GHI from a TMY in NYC .....	27
Figure 15: Average UV Irradiance for Three Selected US Cities .....	27

## List of Tables

Table 1: Solar Irradiance Spectral Categories.....	6
Table 2: Ultraviolet Radiation Spectral Categories.....	6
Table 3: Experimental Results.....	20
Table 4: Model Parameters.....	20
Table 5: Experimental Results for UVA and UVB .....	22
Table 6: Experimental Results for Effect of Sample Thickness .....	23
Table 7: Experimental Results to Test for Reciprocity .....	25
Table 8: Average Irradiance for Selected US Cities .....	28
Table 9: UV Amplification Factor.....	29

## Executive Summary

The aging of asphalt binder due to UV-oxidation is a phenomenon that affects the durability and performance of asphalt pavements. This report documents results of accelerated laboratory UV-oxidation tests that have been conducted. Thin-film asphalt binder samples have been oxidized using fluorescent UVA and UVB lamps, and the degree of oxidation was determined by measuring the rotational viscosity of the aged binder. The results show that the viscosity increases with the UV-exposure time. This indicates that rotational viscosity is a suitable method to track the UV-oxidative aging of asphalt and validates its use in further studies of this phenomenon. Additionally two UV-aging models were fitted to the experimental results.

By comparing the results for the two different types of UV lamps, it was determined that UVA radiation contributes more to the UV-oxidation of asphalt binder than UVB radiation. This is due to UVA radiation comprising a larger portion of the total UV irradiance and the observation that at the same irradiance, UVA radiation causes asphalt binder to both age faster and to reach a higher final viscosity than asphalt aged using UVB radiation. It was determined that the sample thickness plays an important role in UV-oxidation of asphalt binder. An 85% decrease in the thickness caused the aging rate to increase by 52% and the ultimate aging index to increase by 32%. In addition, it was concluded that the UV-oxidation of asphalt binder does not follow the law of reciprocity. Aging at a lower intensity/longer time causes more damage than aging at a higher intensity/shorter time when the product of time and intensity is kept constant.

A UV amplification factor was calculated using information for the global horizontal irradiance for various locations. Compared to a typical meteorological year in New York City, a UVA lamp at an irradiance of  $80 \text{ W/m}^2$ , has an amplification factor of 7.8. This means that each hour of UVA exposure in the lab at  $80 \text{ W/m}^2$  is equivalent to 7.8 hours of in-service UV- exposure.



## **1. Background and Literature Review**

There are several mechanisms that lead to the degradation of asphalt pavements including oxidation of the asphalt binder, fatigue and thermal cracking, raveling, bleeding, and rutting. Oxidation of asphalt binder occurs due to both the high temperatures used during the mixing, transportation, and placement of asphalt pavements (thermal oxidation) and the ultraviolet (UV) radiation found in sunlight that acts throughout the lifetime of the asphalt pavement (UV oxidation). UV radiation produces chemical changes in the asphalt binder, which adversely affect its durability and causes it to become hard and lose strength. During oxidation, asphalt binder begins to stiffen due to the formation of new functional groups including carbonyls and sulfoxides. The chemical changes significantly alter the asphalt binder's rheological properties, including an increase in the viscosity. As this occurs, the asphalt binder becomes more susceptible to fatigue cracks, which will accelerate the degradation of the asphalt pavement.

This process can occur over the course of 5-10 years and laboratory studies aimed at understanding UV-oxidation generally accelerate this process. Accelerated UV-aging is usually accomplished by increasing the intensity of the UV radiation over the typical values that in-service asphalt pavements experience. Various types of lamps can be used including fluorescent, carbon arc, and xenon arc. Carbon arc is an older technology with most current testing using either fluorescent or xenon arc. The difficulty that arises by accelerating the aging process is in determining an acceleration factor that relates the laboratory exposure time with the actual in-service exposure time. An acceleration factor can only be determined after careful evaluation of all of the factors that influence the aging process. These factors include: intensity and spectral distribution of the UV-radiation, asphalt binder thickness and performance grade, the presence of moisture, degree of shading, and temperature.

## 1.1. Solar Radiation

Solar radiation can be divided into the following spectral categories: gamma-rays, X-rays, ultraviolet, visible, infrared, microwave, and radio [1]. The range of wavelengths that comprise each category is given in **Table 1**. The earth's atmosphere absorbs the majority of gamma-rays, x-rays, long-wave radio waves, and infrared. The radiation that reaches the earth's surface is primarily visible light along with some UV and near infrared rays, shown in **Figure 1** [2]. Visible light is divided into the color spectrum (purple, blue, green, yellow, orange, and red) and near infrared has a wavelength range of 760 nm – 1,400 nm. UV radiation is generally divided into the categories shown in **Table 2**.

Extreme-UV and UVC are completely absorbed by the earth's atmosphere, while UVB is mostly absorbed, and UVA is not absorbed. While UVB radiation does contain more energy due to its shorter wavelength, the earth's ozone layer partially stops UVB radiation while allowing UVA radiation to penetrate. The exact spectral distribution of the UVA and UVB portions depends on many factors, including latitude and longitude, the season, time of day, weather, altitude, degree of shading, and levels of atmospheric pollution.

Solar radiation reaches the earth's surface due to two primary mechanisms: direct solar irradiance which arrives to the earth's surface in a straight line from the sun and diffuse solar irradiance which arrives to the earth's surface after being scattered by molecules and particles in the atmosphere. Solar irradiance can be quantified as: direct normal irradiance (DNI), diffuse horizontal irradiance (DIF), and global horizontal irradiance (GHI). All three of these types of solar irradiance are measured in units of power per unit area, typically  $\text{W/m}^2$ . DNI is the amount of solar radiation received by a surface that is held perpendicular to the sun's rays, DIF is the amount of diffuse solar radiation received by a horizontal surface, and GHI is the total amount of

solar radiation (both direct and diffuse) received by a horizontal surface. DNI, DIF, and GHI are related by the following equation:

$$GHI = DIF + DNI \cos \theta \quad \text{Eq. 1}$$

Where  $\theta$  is the solar zenith angle, which is the angle between the sun's rays and a line perpendicular to the earth's surface.

**Table 1: Solar Irradiance Spectral Categories**

Category	Range (nm)
Gamma-Rays	$10^{-5} - 10^{-3}$
X-Rays	$10^{-3} - 10$
Ultraviolet	10 – 400
Visible	380 – 760
Infrared	760 – $10^6$
Microwave	$10^6 - 1.5 \times 10^7$
Radio	$10^6 - 10^{10}$

**Table 2: Ultraviolet Radiation Spectral Categories**

Category	Abbreviation	Range (nm)
Extreme Ultraviolet	EUV	10 – 121
Ultraviolet C	UVC	100 – 280
Ultraviolet B	UVB	280 – 315
Ultraviolet A	UVA	315 – 400

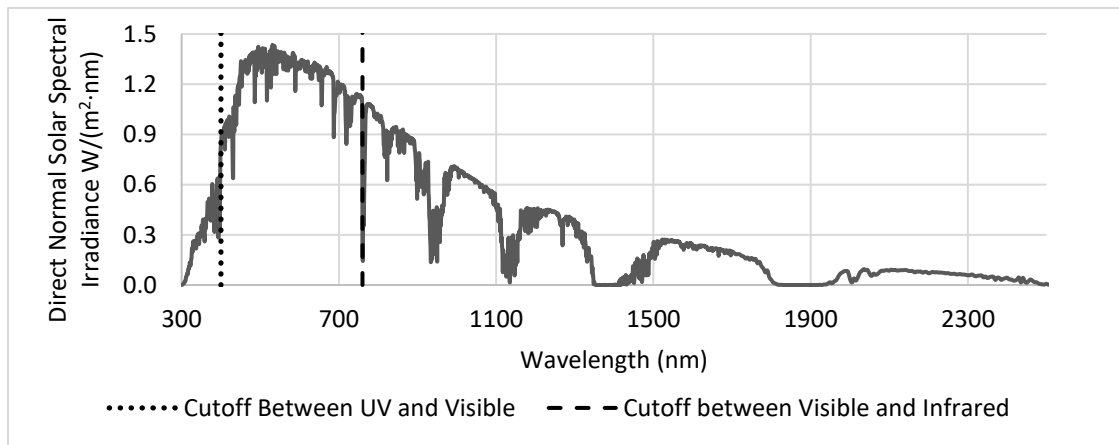


**Figure 1: Reference Solar Spectral Irradiance**

While the solar irradiance is a measurement of the cumulative radiation over all wavelengths that reaches the earth's surface, the solar spectral irradiance describes the solar irradiance per unit wavelength. A solar spectral distribution is a graph which displays the solar spectral irradiance as a function of the wavelength. The exact shape of the spectral distribution depends on many factors, including latitude and longitude, altitude, season of the year, time of day, weather, degree of shading, and levels of atmospheric pollution. A representative solar spectral distribution for direct normal irradiance is given in **Figure 1**, this data is the reference solar spectral irradiance given in ASTM G173 [2]. The GHI in the UV range is computed by integrating the spectral GHI over the range of UV wavelengths:

$$I = \int E(\lambda) d\lambda \quad \text{Eq. 2}$$

Where I is the irradiance,  $E(\lambda)$  is the spectral irradiance, and  $\lambda$  is the wavelength.

## 1.2. Asphalt Oxidation

There are several aging mechanisms that affect asphalt; they include oxidation, volatilization, and physical hardening. That first two are considered irreversible processes because they are produced by changes in the molecular structure, while the latter is reversible because it results from molecular reorganization [3] [4]. Out of these, oxidation is the most important because it contributes significantly to changes in the chemistry and rheology of asphalt. These chemical changes include the formation of carbonyl and sulfoxide compounds, and an increase in the molecular weight [5]. The rheological changes include an increase in the complex modulus and viscosity, and a decrease in the phase angle [6].

Since asphalt binder is an organic material, it will undergo chemical oxidation when it is exposed to atmospheric oxygen. Oxidation hardens asphalt and leads to an overall deterioration in

the desirable physical properties of the material. The hardening that is associated with oxidation will decrease the durability by making asphalt binder more brittle and increasing the susceptibility to cracking. Oxidation results in the introduction of polar, oxygen-containing chemical functional groups into asphalt molecules, which cause increased molecular interactions. Additionally, some aromatization of asphalt molecules may take place. The complexity of the exact chemical reactions and the resulting physicochemical changes that take place are consistent with the complexity of the chemical structure of asphalt binder. Asphalt binder is generally referred to as a polymer-like material; however, the chemical forces that exist at the molecular level are much different than traditional polymers [5].

Most polymers are composed of relatively large molecules of roughly the same chemical formula and molecular weight. Asphalt binder on the other hand is a complex mixture of molecules with differing chemical compositions and molecular weights. These molecules are generally much smaller than the molecules in most polymers; however the polar components of these molecules cluster to form molecular-agglomerates that are of a similar size to typical polymer molecules. The bonds that hold these clusters together are due to polar forces such as hydrogen bonding and dipole interactions. As the temperature is increased, these bonds will break, which will decrease the size of the agglomerates and result in a change in the physical properties. When the temperature is subsequently lowered these bonds will reform. This is due to the reversible nature of these bonds and results in asphalt's temperature-viscosity susceptibility. This link between the nano-level chemical structure and macro-level physical properties is known as physicochemical characterization.

Asphalt binder is primarily composed of the elements hydrogen and carbon; along with the heteroatoms oxygen, sulfur, and nitrogen; and possible trace amounts of vanadium, nickel, and

iron. Due to its complex molecular composition, it is not practical to describe the molecular structure of asphalt in terms of chemical formulae; instead it is generally categorized into four generic fraction components known as the Corbett Fractions [7]. They include saturates, naphthene aromatics, polar aromatics, and asphaltenes. Asphalt can also be categorized into the SARA fractions (saturates, aromatics, resins, and asphaltenes). Saturates are saturated hydrocarbons with little aromaticity and a low heteroatom content that have a low chemical reactivity and a high resistance to oxidation. Aromatics are cyclic (ring-shaped) hydrocarbon molecules. Naphthene aromatics are slightly reactive with oxygen and polar aromatics (resins) are highly reactive with oxygen. Asphaltenes are aromatic in nature and have a high reactivity with oxygen.

Oxidation causes the creation of oxygen-containing functional groups and generally causes a net loss of both naphthene aromatics and polar aromatics, and a net increase in asphaltenes. The primary functional groups that are formed are ketones and sulfoxides, with anhydrides and carboxylic acid (which is also naturally in asphalt binder) being formed in smaller quantities. It has been shown by several researchers [5] [8] [9] [10] that both the amount of ketones and that are formed and the increase in the amount of asphaltenes are linearly related to the log-increase in viscosity. This suggests that the ketones that are formed during oxidation occur on the polar aromatics which form additional asphaltenes.

The viscosity of an asphalt binder results from the complex interactions that take place between the different molecules, with a higher viscosity resulting from more intense interactions. The nonpolar saturates fraction accounts for much of the fluidity of asphalt binder, this is due to the weak interatomic forces that it generates. Griffin et. al [11] measured the viscosity of the saturates, aromatics, and resins fractions to be on the order of 10 Pa-s, 1,000,000 Pa-s, and 1,000,000 Pa-s, respectively. The high viscosity exhibited by the resin fraction is a direct result of

the intense interatomic attraction that it generates due to it being polar aromatic and the presence of heteroatoms. During oxidation the amount of polar functional groups increase, which causes greater intermolecular attraction. This prevents the molecules and molecular-agglomerates from flowing past each other, resulting in decreased molecular-mobility and increased viscosity.

The oxidative aging of asphalt contributes significantly to the degradation of hot mixed asphalt pavements. Standard test methods that are commonly used to evaluate the susceptibility of asphalt to oxidation include the thin film oven test (TFOT) [12], the rolling thin film oven test (RTFO) [13], and the pressure aging vessel (PAV) test [14]. The PAV test simulates the long-term aging of asphalt; however, it does so with increased temperatures and pressure, and not with UV irradiance. The elevated pressure forces air into the asphalt binder which provides the additional oxygen needed to accelerate aging. 20 hours of PAV is equivalent to approximately 5-10 years of long-term in-service aging.

These tests only focus on the effect of temperature on the oxidation process (thermal oxidation) and ignore the contributions from the ultraviolet portion of natural sunlight (photooxidation). This is primarily due to the extremely high temperatures are reached during the mixing, transportation, and placement process and also that only the surface of the asphalt pavement is exposed to sunlight. The consensus had been that the action of sunlight could be ignored since it is only incident on the top surface and asphalt has a high absorption coefficient [15]. Despite work now suggesting that exposure to sunlight does cause degradation that cannot be ignored, standards organizations have not adopted a systematic test for asphalt photooxidation.

### **1.3. Accelerated Photooxidation of Asphalt Binder**

Accelerated UV aging experiments have been conducted by many researchers including Xin et al. [16], Durrieu et al. [17], Feng et al. [6], Wu et al. [18], and Lins et al. [19]. Since there

is no standardized test method, each of these researchers have used slightly different test protocols to both age the asphalt and to evaluate the properties. Xin et al. aged asphalt binder samples that were 635  $\mu\text{m}$  thick, using UVA-340 lamps at an irradiance of  $0.89\text{W}/\text{m}^2$ , in combination with water spray and condensation, at a temperature of  $45^\circ\text{C}$ , and for 100 hours. Durrieu et al. aged asphalt samples that were 10  $\mu\text{m}$  thick, using UVA-340 lamps at an irradiance of  $0.77\text{ W}/\text{m}^2$ , at a temperature of  $60^\circ\text{C}$ , and for 170 hours. Feng et al. aged asphalt samples that were 2 mm thick, using UVA-360 lamps at an irradiance of  $0.80\text{ W}/\text{m}^2$ , at a temperature of  $60^\circ\text{C}$ , and for 72 hours. Wu et al. studied various sample thicknesses (50, 100, 150, and 200  $\mu\text{m}$ ), using UVA-360 lamps at several irradiances (0.95, 1.39, 1.73, and  $2.00\text{ W}/\text{m}^2$ ), at several different temperatures ( $45$ ,  $65$ , and  $80^\circ\text{C}$ ), and for 48 hours of exposure. Lins et al. exposed asphalt samples to a combination of xenon arc lamps and water spray for 2,000 hours of exposure. It can be seen from the above literature survey that there is no standardization for the intensity of the irradiance, wavelength of the lamp, sample dimensions, temperature, or exposure time. Additionally, some researchers have added the effects of moisture and elevated humidity.

The physical properties of the asphalt binder that were studied include needle penetration, softening point, viscosity, ductility, complex modulus, and phase angle. The chemical techniques used include Fourier Transform Infrared Spectroscopy to study the changes associated with carbonyl and sulfoxide groups, thermogravimetric analysis to study the mass gain/loss, and gel permeation chromatography to study changes in the molecular weight.

#### **1.4. Modeling UV-Oxidation of Asphalt Binder**

If UV-oxidation follows the law of reciprocity, which states that the photoresponse of a material is dependent only on the total energy to which the specimen is exposed [20], then UV-oxidative aging is independent of the exposure time and the intensity of the radiation taken



separately. Additionally the radiation dose is then simply the time integral of the irradiance. The law of reciprocity states that the UV radiation dose is computed as:

$$D = \int I dt = \iint E(\lambda) d\lambda dt \quad \text{Eq. 3}$$

If the irradiance is constant throughout the exposure time, then:

$$D = T \int E(\lambda) d\lambda = IT \quad \text{Eq. 4}$$

Where T is the total exposure time. Thus if the law of reciprocity holds true and the irradiance is constant, then the dose of UV radiation is simply the product of the irradiance and the exposure time. If the law of reciprocity is found to be invalid, then Schwarzschild's law can be applied [21]. For a constant irradiance, it states that:

$$D = I^p T \quad \text{Eq. 5}$$

Where p is the Schwarzschild coefficient which is material dependent. If the Schwarzschild coefficient is equal to 1.0, then the law of reciprocity applies.

Since not all wavelengths that are incident on a material are absorbed by the material, and not all absorbed wavelengths cause the same damage to the material, the effective dose of UV radiation is a more complete way to monitor UV exposure. The Lambert-Beer Law specifies the fraction of radiation that is transmitted through (or absorbed by) a material and the Grotthus-Draper Law describes the fraction of photolytically effective photons at each wavelength. For many materials, the wavelength dependency of the Lambert-Beer Law and Grotthus-Draper Law follow the same form and as a result, their combined effect can be described using the action spectrum [22]. The effective UV dose of UV radiation is expressed as:

$$D^* = \iint E(\lambda)H(\lambda)d\lambda dt \quad \text{Eq. 6}$$

where  $D^*$  is the effective dose and  $H(\lambda)$  is the action spectrum of the material. The action spectrum can be further broken down into the product of the spectral absorption and the quantum yield [23].

$$H(\lambda) = (1 - e^{-A(\lambda)})\phi(t) \quad \text{Eq. 7}$$

where  $A(\lambda)$  is the spectral absorbance,  $1 - e^{-A(\lambda)}$  is the spectral absorption, and  $\phi(t)$  is the quantum yield. The spectral absorption quantifies how much each wavelength is absorbed by the material and the quantum yield quantifies what degree each absorbed wavelength damages the material. Using similar reasoning as above, the effective spectral irradiance and effective irradiance and can be defined using Eq. 8 and Eq. 9, respectively:

$$E^*(\lambda) = E(\lambda)H(\lambda) \quad \text{Eq. 8}$$

$$I^*(t) = \int E^*(\lambda) d\lambda = \int E(\lambda)H(\lambda) d\lambda \quad \text{Eq. 9}$$

If the irradiance is constant throughout the exposure and the law of reciprocity applies, then:

$$D^* = T \int E(\lambda)H(\lambda)d\lambda = I^*T \quad \text{Eq. 10}$$

It should be noted that there is some variation in the above terminology, Martin et. al [24] refers to the effective dose as the total effective dosage and to the effective irradiance as the instantaneous effective dosage. Additionally Andradý [23] refers to the effective irradiance as the effective dose rate and to the effective spectral irradiance as the effective irradiance.

### 1.5. Asphalt Aging Models

Several researchers have proposed models to describe asphalt aging [25] [26] [27]. These models have generally been developed to describe the aging of asphalt due to thermal oxidation.

The aging index (AI) is commonly used to quantify the increase in viscosity of an asphalt binder as it is aged:

$$AI = \frac{\eta_A}{\eta_0} \quad \text{Eq. 11}$$

Where  $\eta_0$  is the initial viscosity and  $\eta_A$  is the aged viscosity. The when the asphalt binder is fully aged the AI is known as the ultimate aging index (UAI):

$$UAI = \frac{\eta_{final}}{\eta_0} \quad \text{Eq. 12}$$

Where  $\eta_{final}$ , is the final, fully-aged viscosity.

The Nonlinear Differential Dynamics (NDD) model has been used by Chen and Huang [25] and Garrick [27]. It is based on the Logistics Model that is used to model population growth. The rate of change of the viscosity is given by:

$$\frac{d\eta}{dt} = r\eta(t) - \frac{r}{\eta_{final}}\eta^2(t) \quad \text{Eq. 13}$$

Where  $r$  is the aging rate. By solving the differential equation, the viscosity is given by:

$$\eta(t) = \frac{\eta_{final}}{1 + \left(\frac{\eta_{final}}{\eta_0} - 1\right)e^{-rt}} \quad \text{Eq. 14}$$

The above equation can be written in terms of AI and UAI:

$$AI(t) = \frac{UAI}{1 + (UAI - 1)e^{-rt}} \quad \text{Eq. 15}$$

**Figure 2** illustrates the NDD model and shows the effect of the parameters on the model behavior.

The NDD model assumes that initially there is a rapid increase in the viscosity that eventually levels off to a constant value. Herrington [28] developed the Fast-Rate-Constant-Rate (FRCR) model which models the increase in

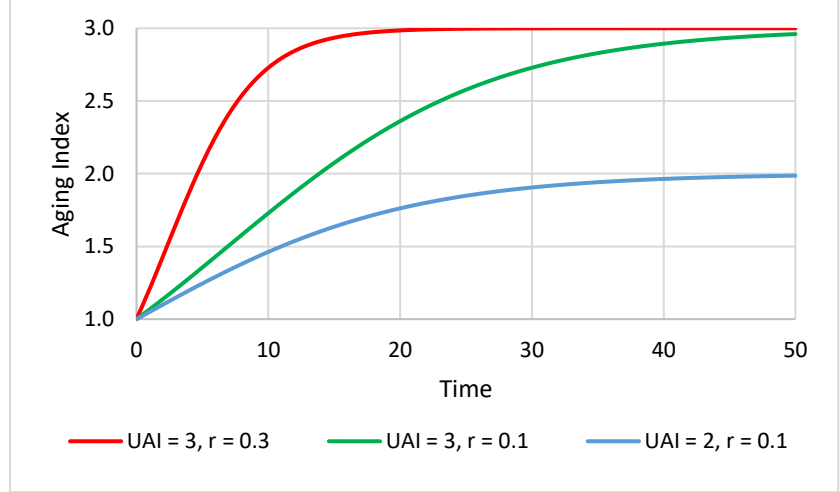


**Figure 2: NDD Model**

the log-viscosity by assuming that oxidation occurs by two parallel reactions, a zero-order reaction and a first-order reaction.

$$\Delta \log \eta = M(1 - e^{-k_2 t}) + kt \quad \text{Eq. 16}$$

Where  $\Delta \log \eta$  is the change of the log-viscosity,  $M$  is the maximum long-term change in the log-viscosity due to the first order reaction,  $k$  is the reaction constant for the zero-order reaction, and  $k_2$  is the reaction constant for the first-order reaction. **Figure 3** illustrates the FRCR model for different values of the parameters. The parameter  $k$  is the slope of the straight-line constant-rate portion and  $M$  is the y-intercept of the straight-line portion if it was extended to a time of zero. Eq. 16 can be written in terms of the aging index:

$$AI = 10^{\Delta \log \eta} = 10^{M(1 - e^{-k_2 t}) + kt} \quad \text{Eq. 17}$$

**Figure 4** illustrates how the AI varies with time using the FRCR model.

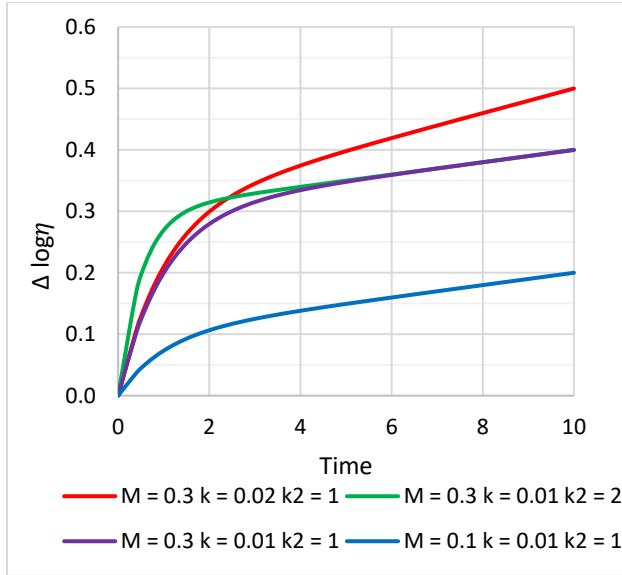


**Figure 3: FRCR Model (Y-Axis is  $\Delta \log \eta$ )**

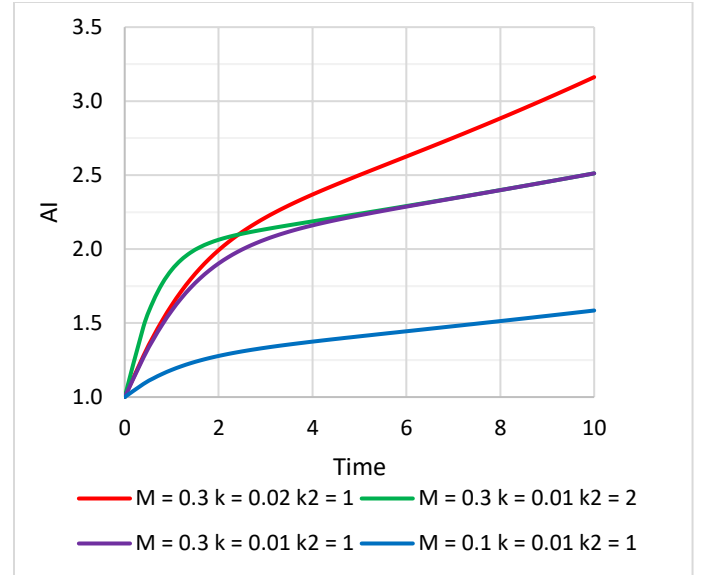


**Figure 4: FRCR Model (Y-Axis is AI)**

## 2. Materials and Methods

### 2.1. Preparation of Asphalt Binder Specimens

The asphalt binder used in this study was a neat roofing flux asphalt. The asphalt binder specimens were prepared as outlined below, which is based on ASTM D1669 [29] with slight modifications. Each specimen consisted of a 5''×2'' asphalt binder layer pressed onto a 6''×3'' bare aluminum (3003-H14) panel, three asphalt binder thicknesses were used in the study (0.1'', 0.075'', and 0.015''). The aluminum panels were prepared by applying masking tape to them so that only a 5''×2'' area is exposed. The masking tape also secured the aluminum panel to a sheet of Kraft paper. The Carver Bench Top Heated Press was then heated to a temperature of 212°F. Next, asphalt binder was heated and poured on to the aluminum panel, which was then placed between the platens of the heated press. A sheet of silicon release paper was placed on top of the asphalt binder and another sheet of Kraft paper was placed between the silicon release paper and the top platen of the heated press. Metal spacers were then placed between the bottom layer of Kraft paper

and the silicon release paper in order to achieve the desired final asphalt thickness. The heated press was then closed and a thrust of 3,500 lb. was applied for 10 seconds.

The asphalt specimen was then removed from the heated press and allowed to cool to room temperature. Once cooled, the silicon release paper was carefully removed to expose the asphalt binder. Using a sharp knife, the asphalt binder was cut along the edges of the masking tape and the excess binder was removed along with the making tape (**Figure 5**). Finally, durable tape was applied around the edges of the asphalt binder to prevent it from flowing during the UV exposure.



**Figure 5: Asphalt Specimen after Masking Tape is Removed**

## **2.2. UV Exposure**

The asphalt binder specimens were exposed to UV radiation using two types of UV lamps, a UVA lamp and a UVB lamp. The intensity of the lamps were measured using a spectrometer and

representative spectral distributions for the two lamps are shown in **Figure 6**. The intensity of the lamps were controlled by adjusting the distance from the lamp to the surface of the asphalt specimen. The intensity of both distributions shown in **Figure 6** is  $80 \text{ W/m}^2$ , with the peak spectral irradiance of the UVA and UVB lamps being  $3.90 \text{ W}/(\text{m}^2 \cdot \text{nm})$  at  $366.5 \text{ nm}$  and  $1.76 \text{ W}/(\text{m}^2 \cdot \text{nm})$  at  $311 \text{ nm}$ , respectively.

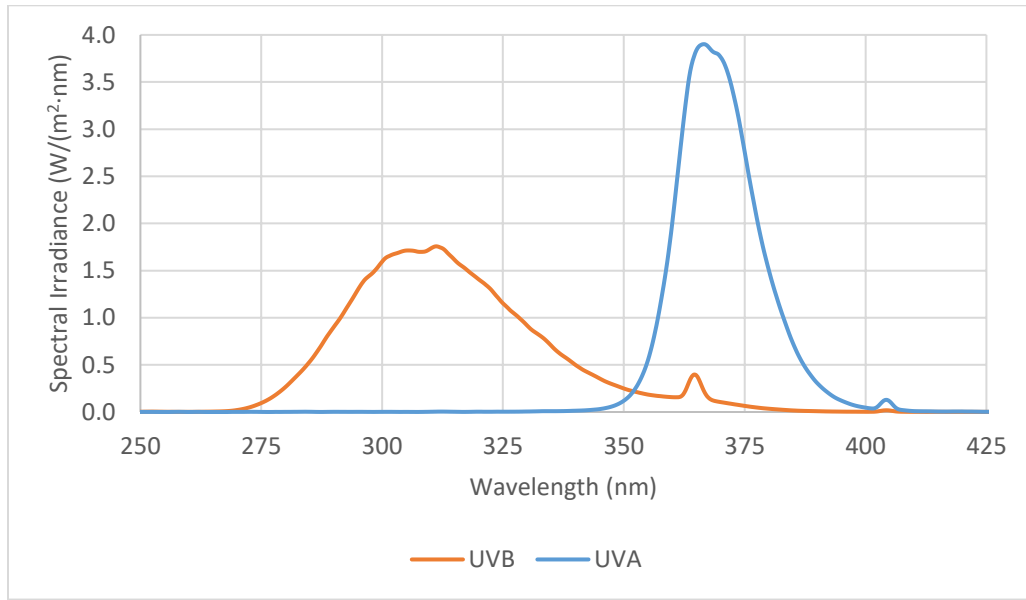


**Figure 6: UV Lamp Spectral Distribution**

### 2.3. Rotational Viscosity of Aged/Unaged Asphalt Binder

The rotational viscosity of the asphalt binder was measured at an elevated temperature according to ASTM D4402 [30] using a rheometer and a thermal chamber. To begin the test, 8 mL of asphalt binder was placed into the sample chamber, after allowing for the temperature of the binder to equilibrate for ten minutes, the SC4-21 spindle was lower into the sample and the spindle was rotated at 20 RPM for 5 minutes in order for the torque readings to stabilize. The viscosity of the asphalt binder was then calculated as the mean value of three consecutive measurements taken at 1-minute intervals. Each viscosity reported in this study is the mean value of two duplicate tests.

### 3. Laboratory Aging Tests

This study has been divided into 4 tasks: 1) evolution of the aging index vs. time, 2) comparison of UVA vs. UVB radiation, 3) effect of sample thickness, and 4) investigation into the reciprocity of intensity/time.

#### 3.1. Aging Index vs. Time

Thin-film asphalt binder samples with a thickness of 0.075” were aged using a UVA lamp with an intensity of 80 W/m<sup>2</sup>. The asphalt used was a roofing flux and the rotational viscosity was measured at a temperature of 135°C, using a SC4-21 spindle, and at 20 RPM. Samples were exposed to UVA radiation for exposure times of 5, 10, 20, 30, and 50 hours and the rotational viscosity of each binder sample was measured using a rotational viscometer. The results are displayed in **Table 3** along with the value of the aging index. **Figure 7** displays the average viscosity/aging index at each exposure time and **Figure 8** displays the fitted NDD and FRCR models to the experimental data. The values of the determined model parameters are shown in **Table 4**. Overall both models appear to be able to describe the evolution of the aging index as a result of UV-oxidation.

Overall the viscosity increased with UV exposure time, indicating that UV oxidation is taking place. The NDD model predicts that the UAI is 1.34, which is lower than literature values for both thermal oxidation and UV oxidation. Both Garrick [27] and Chen and Huang [25] determined the UAI of field aged asphalt binder by extracting the binder from road cores. Garrick reported UAI values between 3.3 and 5.0 after 4 years of aging and Chen and Huang reported UAI values between 1.9 and 2.4 after 3 years of aging. The experimental results indicate that, despite the AI vs. time curve leveling off, the asphalt binder was not fully aged since its UAI is



significantly lower than reported values. This is most likely due to the nonuniform oxidation of the asphalt binder in the depth direction.

**Table 3: Experimental Results**

Time (hrs)	Average Viscosity (cP)	Aging Index
0	393	1.00
5	500	1.27
10	513	1.31
20	529	1.35
30	520	1.32
50	537	1.37

**Table 4: Model Parameters**

Model	Parameter	Value
NDD	UAI	1.34
	r	0.338 hr <sup>-1</sup>
FRCR	M	0.117
	k <sub>2</sub>	0.405 hr <sup>-1</sup>
	k	3.50x10 <sup>-4</sup> hr <sup>-1</sup>

### 3.2. UVA vs. UVB

It is important to compare the UV-oxidation of asphalt binder using UVA and UVB radiation for two reasons. Since UVA and UVB radiation contain different wavelength of electromagnetic radiation, they will have different effects on the resulting physicochemical changes that take place. Additionally the spectral distribution of natural sunlight contains different amounts of UVA and UVB radiation.

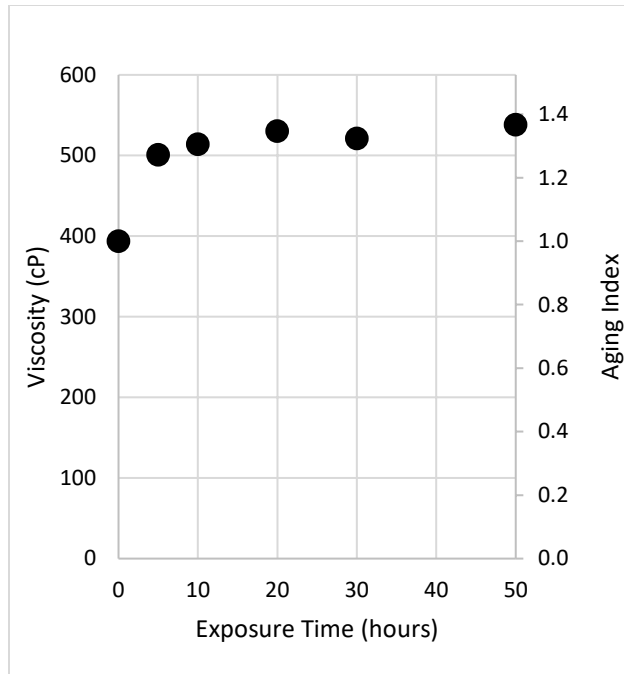


**Figure 7: Experimental Results**

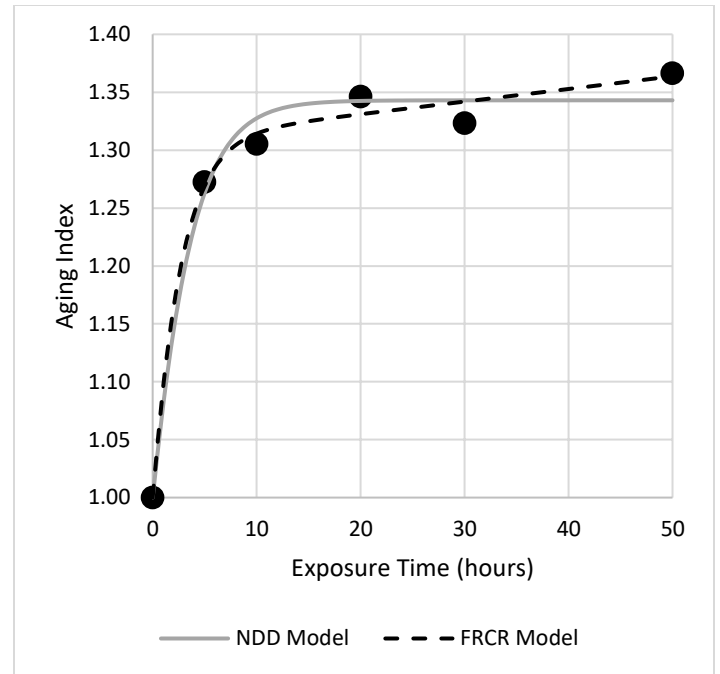


**Figure 8: NDD and FRCR Models Fitted to Experimental Results**

Asphalt binder samples with a thickness of 0.1” were exposed to UV-radiation with an intensity of  $80 \text{ W/m}^2$  for durations of 20, 50, and 100 hours using either UVA or UVB lamps. The rotational viscosity of the aged asphalt binder was measuring using a rotational viscometer at a temperature of  $100^\circ\text{C}$ , using a SC4-21 spindle, and at a speed of 20 RPM. The results are shown in **Table 5** and **Figure 9**, additionally the data was fitted using the NDD aging model. From the results, the UVA samples have both a higher aging rate ( $0.063 \text{ vs. } 0.029 \text{ hr}^{-1}$ ) and ultimate aging index ( $1.11 \text{ vs. } 1.07$ ) than the UVB samples. It is observed that, when exposed to the same intensity of UVA and UVB radiation, asphalt binder subjected to UVA radiation both receives more damage and ages faster than asphalt binder subjected to UVB radiation.

### 3.3. Effect of Sample Thickness

It has been shown by Wu et al. [18] that the asphalt film thickness has a significant influence on the amount of UV-oxidation that occurs. A study conducted by Kiil [31] has shown

that photo-initiated oxidation of thin samples depends on the rate of chemical oxidation, the solubility of oxygen in the coating, and the rate of diffusion of oxygen into the coating. The study also showed that there exists two regions, one is the oxidation zone where oxidation is occurring and the other is the inactive zone where oxidation is not occurring.

**Table 5: Experimental Results for UVA and UVB**

Time (hrs)	UVA		UVB	
	$\eta$ (cP)	AI	$\eta$ (cP)	AI
0	358	-	358	-
20	383	1.07	363	1.01
50	399	1.11	383	1.07
100	394	1.10	379	1.06
$r$ ( $\text{hr}^{-1}$ )	0.063		0.029	
UAI	1.11		1.07	

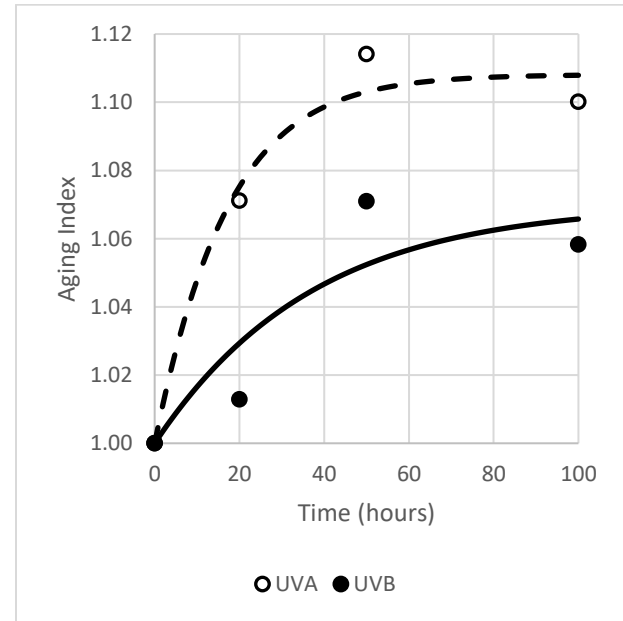


**Figure 9: Aging Index for UVA and UVB**

Roofing flux samples with a thickness of 0.015” were exposed to UV-radiation with an intensity of  $80 \text{ W/m}^2$  for durations of 24 and 48 hours using UVA lamps. The rotational viscosity of the aged asphalt binder was measuring using a rotational viscometer at a temperature of  $100^\circ\text{C}$ , using a SC4-21 spindle, and at a speed of 20 RPM. The results of these samples are compared to the UVA samples described in the previous section that had a thickness of 0.1” and were aged according to the same procedure. The results comparing the two thicknesses are shown in **Table 6** and **Figure 10**, additionally the data was fitted using the NDD aging model.

The results indicate that the thinner samples have both a higher aging rate (0.096 vs. 0.063  $\text{hr}^{-1}$ ) and ultimate aging index (1.47 vs. 1.11) than the thicker samples. It is observed that, when

exposed to the same intensity of UVA radiation, a thinner layer of asphalt binder both receives more damage and ages faster. From the results, an 85% decrease in the thickness caused the aging rate to increase by 52% and the ultimate aging index to increase by 32%.

**Table 6: Experimental Results for Effect of Sample Thickness**

0.1" Thickness			0.015" Thickness		
Time (hrs)	$\eta$ (cP)	AI	Time (hrs)	$\eta$ (cP)	AI
0	358	-	0	358	-
20	383	1.07	24	504	1.41
50	399	1.11	48	525	1.47
100	394	1.10	-	-	-
r (hr <sup>-1</sup> )	0.063		r (hr <sup>-1</sup> )	0.096	
UAI	1.11		UAI	1.47	

### 3.4. Reciprocity of Time/Intensity

The law of reciprocity relies on the assumption that the amount of photooxidation depends only on the total absorbed energy (product of intensity and time) and not on the values of the time and intensity taken separately. If the value of the Schwarzschild coefficient in Eq. 5 is equal to 1.0, then the law of reciprocity applies. If the coefficient is lower than 1.0, then UV-aging for a longer period of time at a lower intensity is more damaging than UV-aging for a shorter period of time at a higher intensity. If the coefficient is greater than 1.0, then the opposite is true. Thus determining a value of the Schwarzschild coefficient is extremely important because the intensity of natural

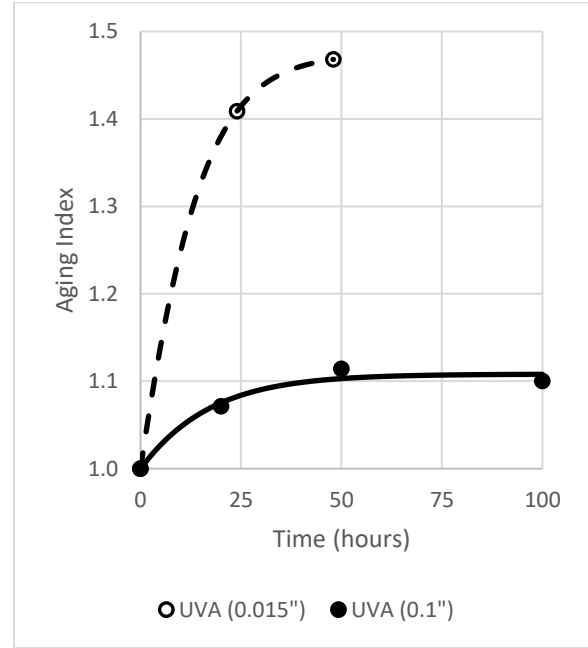


**Figure 10: Aging Index for Different Sample Thicknesses**

UV radiation varies and accelerated UV-aging is conducted at intensities that are higher than natural UV radiation.

In order to determine the value of the Schwarzschild coefficient, asphalt samples were aged using the same amount of energy, but for different times and at different intensities. The first exposure condition was an intensity of 80 W/m<sup>2</sup> for 24 hours and the second exposure condition was an intensity of 40 W/m<sup>2</sup> for 48 hours. For both exposures, the product of time and intensity is 6.91 MJ/m<sup>2</sup>. The tests were repeated for both UVA and UVB radiation using samples with a thickness of 0.015". The asphalt used was a roofing flux and the rotational viscosity was measured at a temperature of 100°C, using a SC4-21 spindle, and at 20RPM. As seen in **Table 7**, for both UVA and UVB exposure, the lower intensity/longer time exposure condition resulted in a larger aging index than the higher intensity/shorter time exposure condition, thus the law of reciprocity does not apply. The value of the Schwarzschild coefficient can be determined by the following equation:

$$p = \log_2 \left( \frac{2AI_1}{AI_2} \right) \quad \text{Eq. 18}$$

Where AI<sub>1</sub> is the aging index for the shorter time/higher intensity and AI<sub>2</sub> is the aging index for the longer time/lower intensity. The value of Schwarzschild coefficient for both UVA and UVB exposures is lower than 1.0, at 0.82 and 0.83, respectively.

#### **4. Estimation of the In-Service UV Radiation Dose**

A Typical Meteorological Year (TMY) is a dataset that contains representative data for the DNI and GHI for a given location, as well as other meteorological data such as ambient temperature, wind speed, etc. TMY data is generally used for long-term predictions. Sources for TMY data include the program Meteonorm developed by Meteotest and the National Solar

Radiation Database (NSRDB) created by the National Renewable Energy Lab (NREL). The NSRDB is a web-based technical report that provides hourly solar and meteorological data for over 1,400 locations in the United States and its territories [32].

**Table 7: Experimental Results to Test for Reciprocity**

UV Type	Time (hr)	Intensity (W/m <sup>2</sup> )	$\eta$ (cP)	AI	p
-	0	-	358.0	-	-
UVA	24	80	493.3	1.38	0.82
	48	40	558.3	1.56	
UVB	24	80	407.5	1.14	0.83
	48	40	458.3	1.28	

#### 4.1. UV Irradiance for Selected US Cities

**Figure 11** displays the noon spectral GHI in the UV range for a TMY at LaGuardia Airport in New York City. This data is shown for 4 dates: 3/21, 6/21, 9/21, and 12/21; the approximate dates for the vernal equinox, summer solstice, autumnal equinox, and winter solstice, respectively. This illustrates the seasonal variation of the UV

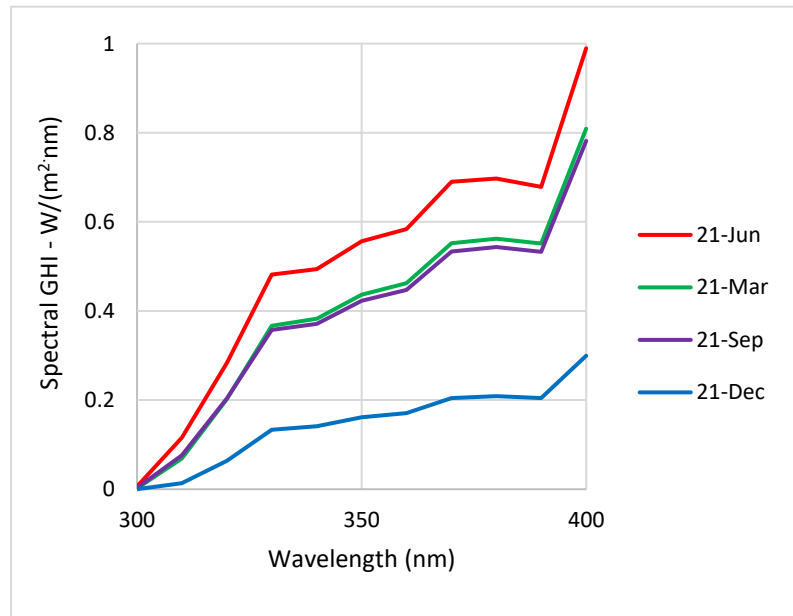


**Figure 11: Noon Spectral GHI for LGA**

spectral distribution that is experienced. **Figure 12** and **Figure 13** show the spectral GHI in the UV range for a TMY in New York City at two hour intervals for 6/21 and 12/21, respectively. Here it is observed that UV spectral distribution varies considerably based on the time of day. Additionally the spectral distribution at noon during the winter is only slightly higher than the spectral distribution that is experienced at 6:00 am during the summer.

**Figure 14** displays how the total UV irradiance in New York City varies throughout the day for 4 selected dates from a TMY. The total UV irradiance is calculated by applying Eq. 2 to the spectral distribution of the GHI in the UV range. This further illustrates both the seasonal and hourly variation in the UV exposure. **Figure 15** displays the average UV irradiance each month for three US cities, New York City, Denver, and Phoenix. The data in this figure was generated by averaging the hourly UV irradiance over a month. **Table 8** displays the average UV irradiance (calculated by averaging over an entire TMY) for the same three US cities. This illustrates that the UV irradiance is additionally dependent on geographic location. The average daily UV irradiance in Denver and Phoenix are 24% and 45% larger than the average daily UV irradiance experienced in New York City. Additionally this table contains the percentage of the average UV irradiance that is within the UVA range (the remaining percentage is within the UVB range). Combining the information contained in **Table 5** and **Table 8**; it can be concluded that UVB radiation does not significantly contribute to the UV-aging of asphalt binder. This is because at the same irradiance UVA causes almost double the amount of damage as UVB and natural sunlight contains approximately 49 times more energy in the UVA range than in the UVB range. As a result, the following analysis will only account for UVA radiation.

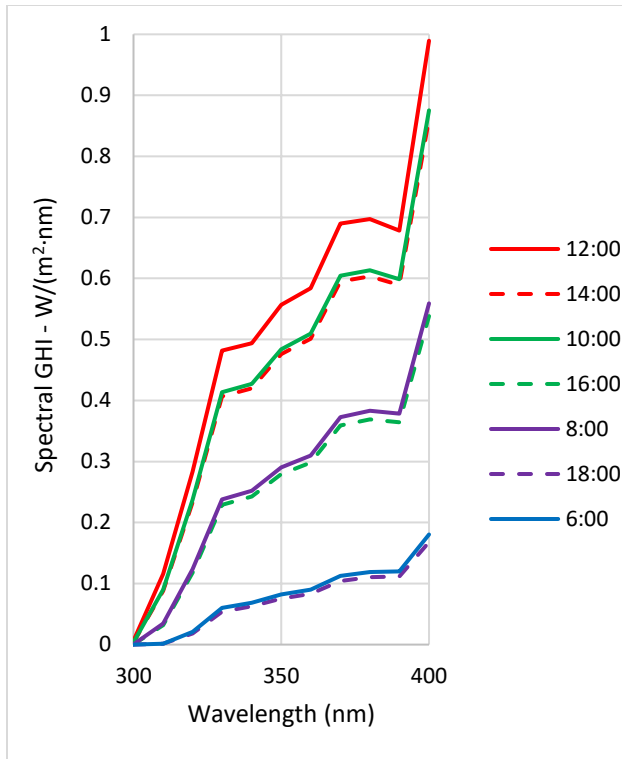


**Figure 12: Spectral UV GHI from a TMY in NYC - 6/21**

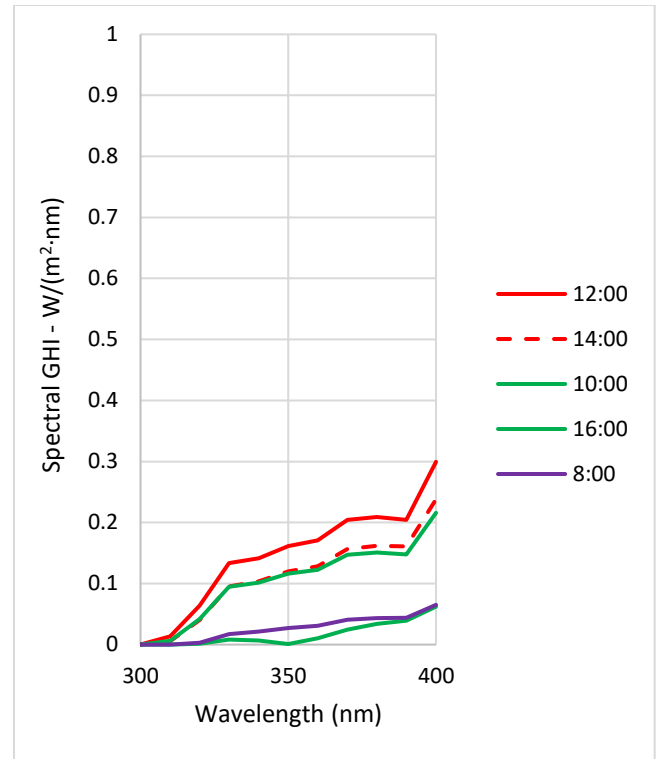


**Figure 13: Spectral UV GHI from a TMY in NYC - 12/21**

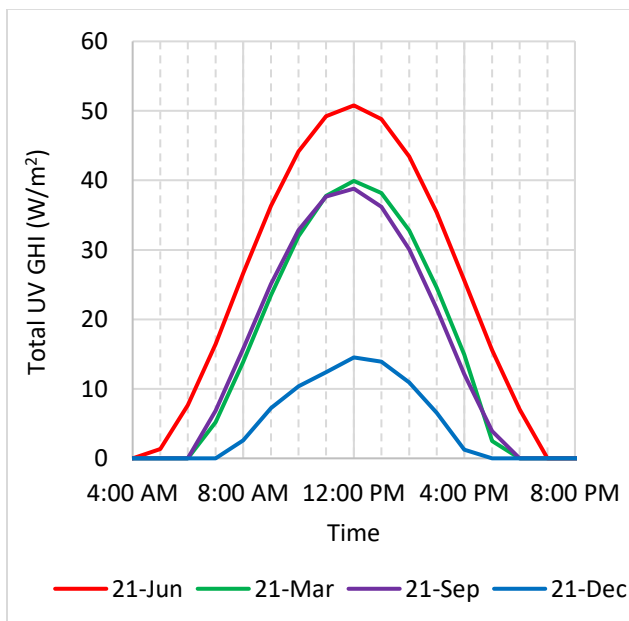


**Figure 14: Total UV GHI from a TMY in NYC**

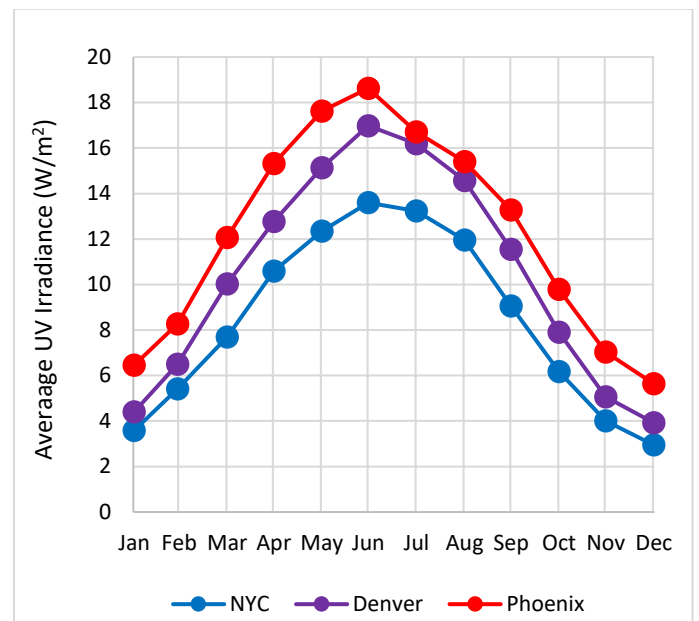


**Figure 15: Average UV Irradiance for Three Selected US Cities**



**Table 8: Average Irradiance for Selected US Cities**

<b>City</b>	<b>Average UV Irradiance (W/m<sup>2</sup>)</b>	<b>Average UVA Irradiance (W/m<sup>2</sup>)</b>	<b>% UVA</b>
New York City	8.4	8.2	98.0
Denver	10.4	10.2	98.0
Phoenix	12.2	11.9	97.8

#### **4.2. Correlation between Laboratory and In-Service UV Aging**

The asphalt aging acceleration factor relates the laboratory UV aging with the in-service aging that asphalt experiences. The numerical value of the acceleration factor is dependent on many variables including the spectral distribution of the laboratory UV source and the geographic location, weather, and degree of shading (from buildings, trees, etc.) at the location where the in-service aging is occurring. This study has accounted for both the spectral distribution of the laboratory UV source and the geographic location of the in-service aging; however, it does not account for the weather and the degree of shading. It has been concluded by Xin et al. [16] that the action of water spray during UV exposure slows down the rate of UV-oxidation, while Ongel and Hugener [33] have concluded that an increase in the relative humidity slows down the asphalt aging process. While the TMY data that has been used to calculate average UV irradiance accounts for cloud cover that reduces the GHI, it does not account for the reduction in UV-oxidation that occurs from water on the surface of the asphalt and the relative humidity of the air. As a result, only a UV amplification factor can be calculated from the data collected in this study. The UV amplification factor only relates UV radiation that is produced in the laboratory with the UV radiation at a specific geographic location. This factor does not account for presence of moisture and degree of shading, however it does account for the differences in the spectral distribution

between the two UV sources and also for the effect that the magnitude of the UV irradiance has on the rate of aging (i.e. reciprocity is not valid). **Table 9** contains the UV amplification factor for selected US cities calculated using the following equation:

$$AF = \frac{\sum(I_{lamp,UVA})^p}{\sum(I_{hourly,UVA})^p} \quad \text{Eq. 19}$$

Where  $I_{lamp,UVA}$  is the irradiance of the laboratory UVA lamp and  $I_{hourly,UVA}$  is the UVA irradiance each hour in a TMY. The summation is over the number of hours in a year. For comparison purposes the table also displays the value of the amplification factor if the law of reciprocity did apply ( $p = 1$ ). To illustrate the use of the amplification factor, one day of exposure in the laboratory using a UVA lamp at an irradiance of  $80 \text{ W/m}^2$  is equivalent to 7.8 average days of exposure in New York City. During the summer and winter, the amplification factor will be lower and higher, respectively, due to the seasonal variation in the natural UV irradiance. Additionally **Table 9** contains the total annual UVA dose for the three US cities, these number can be compared to the UVA lamp at an irradiance of  $80 \text{ W/m}^2$ , which has an annual dose of  $1146 \text{ MJ/m}^2$

**Table 9: UV Amplification Factor**

City	UV Amplification Factor of a 80 W/m <sup>2</sup> UVA Lamp		Annual UVA Dose (MJ/m <sup>2</sup> )	
	Reciprocity	No Reciprocity	Reciprocity	No Reciprocity
New York City	9.7	7.8	260	148
Denver	7.8	6.5	323	178
Phoenix	6.7	5.6	376	203

## 5. Conclusions

This study successfully accelerated the aging of asphalt binder due to UV-oxidation using fluorescent UV lamps in the laboratory. The aging index of the asphalt binder was determine by

measuring the viscosity using a rotational viscometer and two asphalt oxidation models were fitted to the experimental data. The following conclusions can be reached concerning the photooxidation of asphalt binder using UV-radiation.

1. The rotational viscosity is an appropriate technique to measure the aging of asphalt binder due to UV-oxidation. It has been demonstrated that the rotational viscosity of asphalt binder increases along with the UV-exposure time. Additionally both the Nonlinear Differential Dynamics (NDD) model and the Fast-Rate-Constant-Rate (FRCR) model are able to effectively capture the evolution of the aging index with respect to the exposure time.
2. UVB radiation does not significantly contribute to the UV-aging of asphalt binder. This is because:
  - a. At the same irradiance UVA causes almost double the amount of damage as UVB. This is based on calculating the ultimate aging index and aging rate using the NDD model.
  - b. Natural sunlight contains approximately 49 times more energy in the UVA range than in the UVB range.
3. Thinner asphalt samples receive more damage and age faster than thicker asphalt samples. A decrease in the thickness from 0.1” to 0.015” caused an increase in both the aging rate (0.063 to 0.096 hr<sup>-1</sup>) and ultimate aging index (1.11 to 1.47).
4. The law of reciprocity does not apply to the UV-aging of asphalt binder. For the asphalt binder tested in this study  $p = 0.82$  for UVA and  $p = 0.83$  for UVB. This indicates that a lower intensity/longer time exposure condition results in faster aging than a higher intensity/shorter time exposure condition. In other words, doubling the intensity of the UV source does not double the amount of UV-aging.

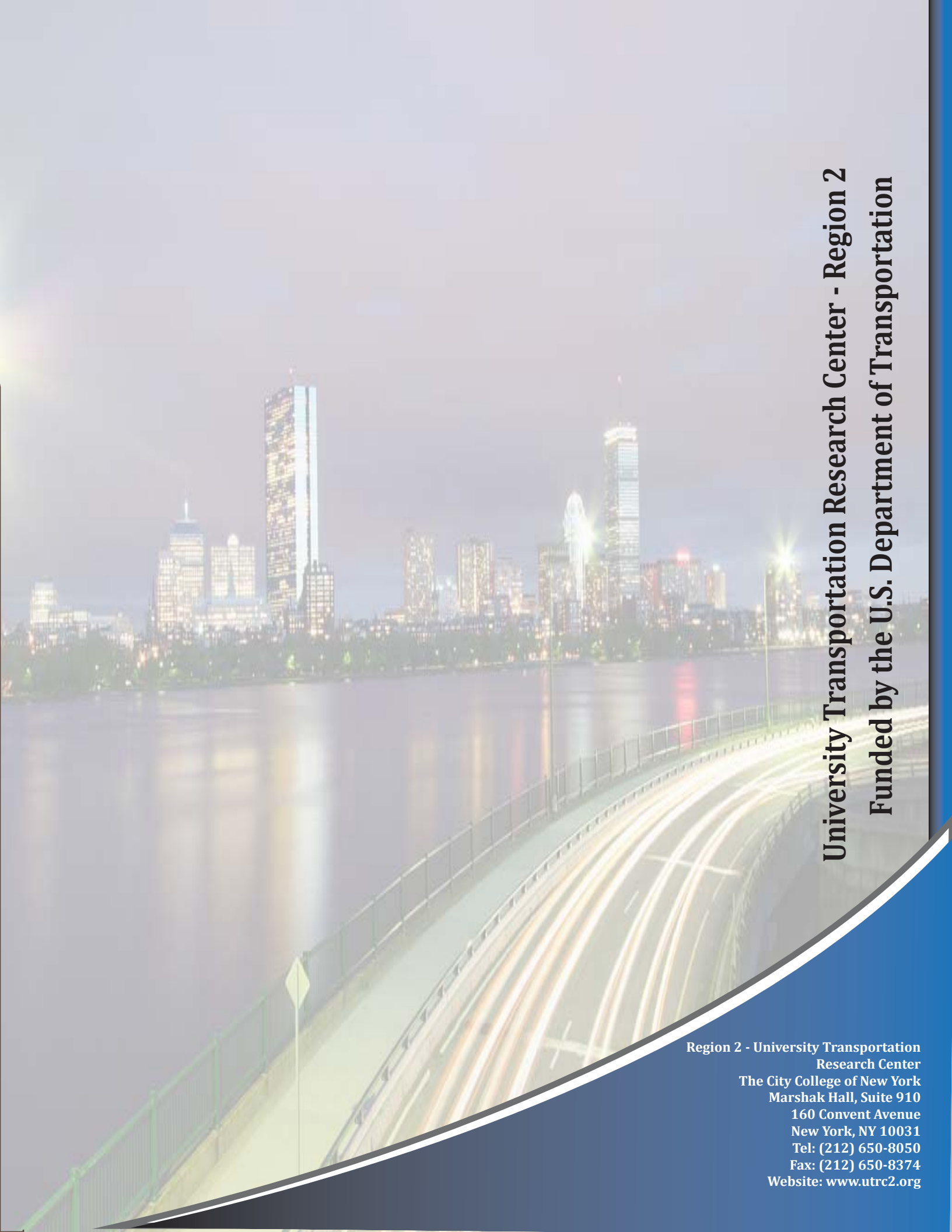
5. The amplification factor for UV aging using a UVA lamp with an irradiance of  $80 \text{ W/m}^2$  is 7.8 for New York City, 6.5 for Denver, and 5.6 for Phoenix. This amplification factor is based on the ratio of the annual dose of UVA radiation that an asphalt sample receives from the UVA lamp to the annual dose of UVA radiation that the same sample would receive in a year at the various locations. The amplification factor assumes that the asphalt binder is not shaded and is exposed to the entire global horizontal irradiance.

## References

- [1] ISO 21348: Space Environment (Natural and Artificial) - Process for Determining Solar Irradiances, Geneva, Switzerland, 2007.
- [2] ASTM International, ASTM G173: Standard Table for Reference Solar Spectral Irradiances: Direct Normal and Hemispherical on 37° Tilted Surface, West Conshohocken, PA, 2012.
- [3] C. Bell, "Summary report on the aging of asphalt-aggregate systems," *Transportation Research Board*, 1989.
- [4] X. Lu and U. Isacson, "Effect of ageing on bitumen chemistry and rheology," *Construction and Building Materials*, vol. 16, no. 1, pp. 15-22, 2002.
- [5] J. C. Petersen, "A Review of the Fundamentals of Asphalt Oxidation: Chemical, Physicochemical, Physical Property, and Durability Relationships," *Transportation Research E-Circular*, Vols. E-C140, 2009.
- [6] Z. G. Feng, J. Y. Yu, H. L. Zhang, D. L. Kuang and L. H. Xue, "Effect of ultraviolet aging on rheology, chemistry and morphology of ultraviolet absorber modified bitumen," *Mater. Struct.*, vol. 46, no. 7, pp. 1123-1132, 2012.
- [7] L. W. Corbett, "Composition of Asphalt Based on Generic Fractionation, Using Solvent Deasphalting, Elution-Adsorption Chromatography, and Densimetric Characterization," *Analytical Chemistry*, vol. 41, no. 4, pp. 576-579, 1969.
- [8] C. K. Lau, K. M. Lunsford, C. J. Glover, R. R. Davison and J. A. Bullin, "Reaction Rates and Hardening Susceptibilities as Determined from Pressure Oxygen Vessel Aging of Asphalts," *Transportation Research Record*, vol. 1342, 1992.
- [9] K. L. Martin, R. R. Davison, C. J. Glover and J. A. Bullin, "Asphalt Aging in Texas Roads and Test Sections," *Transportation Research Record*, vol. 1269, 1990.
- [10] J. C. Petersen, J. F. Branthaver, R. E. Robertson, P. M. Hamsberger, J. J. Duvall and E. K. Ensley, "effects of Physicochemical Factors on Asphalt Oxidation Kinetics," *Transportation Research Record*, vol. 1391, 1993.
- [11] R. L. Griffen, W. C. Simpson and T. K. Miles, "Influence of Composition of Paving Asphalts on Viscosity, Viscosity-Temperature Susceptibility, and Durability," *Journal of Chemistry and Engineering Data*, vol. 4, pp. 349-354, 1959.
- [12] ASTM International, "ASTM D1754: Standard Test Method for Effects of Heat and Air on Asphaltic Materials (Thin-Film Oven Test)," West Conshohocken, PA, 2014.

- [13] ASTM International, "ASTM D2872: Standard Test Method for Effect of Heat and Air on a Moving Film of Asphalt (Rolling Thin-Film Oven Test)," West Conshohocken, PA, 2012.
- [14] ASTM International, "ASTM D6521: Standard Practice for Accelerated Aging of Asphalt Binder Using a Pressure Aging Vessel (PAV)," West Conshohocken, PA.
- [15] G. D. Airey, "State of the Art Report on Ageing Test Methods for Bituminous Pavement Materials," *Int. J. Pavement Eng.*, vol. 4, no. 3, pp. 165-176, 2003.
- [16] H. Xin, D. Hochstein, Q. Ge, A. W. Ali, F. Chen and H. Yin, "Accelerated Aging of Asphalt by UV Photo-Oxidation Considering Moisture and Condensation Effects," *Journal of Materials in Civil Engineering*, vol. 30, no. 1, 2018.
- [17] F. Durieu, F. Farcas and V. Mouillet, "The influence of UV aging of a styrene/butadiene/styrene modified bitumen: Comparison between laboratory and on site aging," *Fuel*, vol. 86, no. 10-11, pp. 1446-1451, 2007.
- [18] S. Wu, L. Pang, G. Liu and J. Zhu, "Laboratory Study on Ultraviolet Radiation Aging of Bitumen," *J. Mater. Civ. Eng.*, vol. 22, pp. 767-772, 2010.
- [19] V. F. Lins, M. F. A. S. Araujo, M. I. Yoshida, V. P. Ferraz, D. M. Andrada and F. S. Lameiras, "Photodegradation of hot-mixed asphalt," *Fuel*, vol. 87, no. 15-16, pp. 3254-3261, 2008.
- [20] J. Chin, T. Nguyen, E. Byrd and J. Martin, "Validation of the reciprocity law for coating photodegradation," *J. Coatings Technol. Res.*, vol. 2, no. 7, pp. 499-508, 2005.
- [21] K. Schwarzschild, "On the derivations from the law of reciprocity for bromide of silver gelatine," *Am. Astron. Soc.*, vol. 11, pp. 89-91, 1900.
- [22] J. Martin, J. Lechner and R. Varner, "Accelerated outdoor durability testing of organic materials," *ASTM STP 1202*, 1994.
- [23] A. L. Andraday, "Wavelength Sensitivity in Polymer Photodegradation," in *Polymer Analysis Polymer Physics*, Springer-Verlag Berlin Heidelberg, 1997, pp. 47-94.
- [24] J. W. Martin, J. A. Lechner and R. N. Varner, "Quantitative Characterization of Photodegradation Effects of Polymeric Materials Exposed in Weathering Environments," in *Accelerated and Outdoor Durability Testing of Organic Materials*, ASTM International, 1994.
- [25] J. S. Chen and L. S. Huang, "Developing an Aging Model to Evaluate Engineering Properties of Asphalt Paving Binders," *Materials and Structures*, vol. 33, no. 9, pp. 559-565, 2000.

- [26] X. Jin, R. Han, Y. Cui and C. J. Glover, "Fast-Rate–Constant-Rate Oxidation Kinetics Model for Asphalt Binders," *Industrial and Engineering Chemistry Research*, vol. 50, no. 23, pp. 13373-13379, 2011.
- [27] N. W. Garrick, "Nonlinear Differential Equation for Modeling Asphalt Aging," *Journal of Materials in Civil Engineering*, vol. 7, no. 4, pp. 265-268, 1995.
- [28] P. R. Herrington, "Oxidation of Bitumen in the Presense of a Constant Concentration of Oxygen," *Petroleum Science and Technology*, vol. 16, no. 7-8, pp. 743-765, 1998.
- [29] ASTM International, "ASTM D1669: Standard Practice for Preparation of Test Panels for Accelerated and Outdoor Weathering of Bituminous Coatings," West Conshohocken, PA, 2013.
- [30] ASTM International, "ASTM D4402: Standard Test Method for Viscosity Determination of Asphalt at Elevated Temperatures Using a Rotational Viscometer," West Conshohocken, PA, 2015.
- [31] S. Kiil, "Model-based analysis of photoinitiated coating degradation under artificial exposure conditions," *J. Coatings Technol. Res.*, vol. 9, no. 4, pp. 375-398, 2012.
- [32] NREL, "NSRDB Data Viewer," [Online]. Available: <https://maps.nrel.gov/nsrdb-viewer>. [Accessed 1 July 2017].
- [33] A. Ongel and M. Hugener, "Aging of Bituminous Mixtures for RAP Simulation," *Construction and Building Materials*, vol. 68, pp. 49-54, 2014.



# University Transportation Research Center - Region 2

## Funded by the U.S. Department of Transportation

Region 2 - University Transportation  
Research Center  
The City College of New York  
Marshak Hall, Suite 910  
160 Convent Avenue  
New York, NY 10031  
Tel: (212) 650-8050  
Fax: (212) 650-8374  
Website: [www.utrc2.org](http://www.utrc2.org)